J Mater Sci (2007) 42:3349–3352
DOI 10.1007/s10853-006-1169-2

SIZE-DEPENDENT EFFECTS

Influence of the synthesis methods on the particle size of the $LiVMoO_6$ phase

**Margarita Milanova · Reni Iordanova ·
Yanko Dimitriev · Krassimir Kostov ·
Sasho Vassilev**

Received: 1 June 2006 / Accepted: 20 October 2006 / Published online: 27 March 2007

Abstract The lithiated transition metal oxide $LiVMoO_6$ has been synthesized by a novel melt quenching method that presents some advantages as compared to the classical solid-state reaction and soft-combustion synthesis. These are: the short preparation time and the possibility to control the grain size of $LiVMoO_6$ powders. The local structure of $LiVMoO_6$ samples prepared in different ways was characterized by IR spectral analysis. The oxidation state of Li, V, and Mo was determined by X-ray photoelectron spectroscopy.

Introduction

A new 4V-class lithiated transitional metal oxide, $LiVMoO_6$, recently attracted special attention as an electrode—active material in rechargeable lithium ion batteries. Since the electrochemical features of this material depend on their crystal nature, size and shape, five different variations of a conventional solid state reaction [1–3] and wet chemistry technique (sol–gel, soft-combustion synthesis and rheological phase reaction) [2, 4, 5] have been developed to improve its characteristics. Our experience in the synthesis of vanadate and molybdate phases has provoked extension of the experimental manners for $LiVMoO_6$ preparation by two new methods—melt quenching and crystallization of a glass. It was aimed at comparing different preparative ways for obtaining $LiVMoO_6$ and their peculiarities.

Experimental

Figure 1 schematically illustrates the methods and preparation steps adopted for the synthesis of $LiVMoO_6$. As is seen from the figure, five manners were used to produce the phase. Solid-state reaction (method A) and soft-combustion synthesis (method B) were applied following the procedure described in [1–4]. $LiVMoO_6$ was obtained also by melt quenching at different rates (method C—cooling rate 10^3 K/s and D—cooling rate 10^4–10^5 K/s), and crystallization of a glass (method E). Glasses were prepared using reagent grade Li_2CO_3, V_2O_5 and MoO_3 as starting compounds. The homogenized batches were melted for 10 min. in air in alumina crucibles at 600–800 °C depending on the melting temperatures of the compositions. Owing to the high crystallization tendency of the melts, high cooling rates (10^4–10^5 K/s) were applied using the roller-quenching method in order to define the glass formation region. Only fragmented 1–3 cm flat pieces, about 50–100 μm thick, were produced. By visual observation it was assumed that those compositions, in which vitreous pieces are above 2/3 of the samples, were identified as glasses.

M. Milanova (✉) · R. Iordanova · K. Kostov
Institute of General and Inorganic Chemistry, Bulgarian Academy of Sciences, 1113 Sofia, Bulgaria
e-mail: margi71@abv.bg

Y. Dimitriev
University of Chemical Technology and Metallurgy, Sofia 1756, Bulgaria

S. Vassilev
Institute of Electrochemistry and Energy Systems, 1113 Sofia, Bulgaria

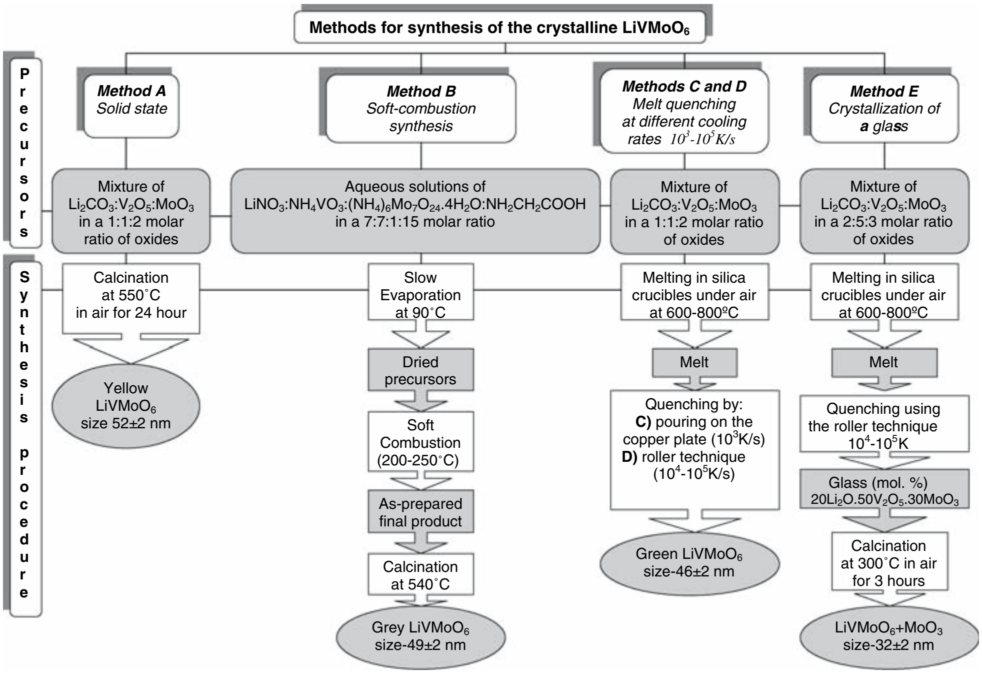

Fig. 1 Schematically representation of the methods and preparation steps adopted to obtain of crystalline $LiVMoO_6$

Powder XRD patterns of the sample obtained by all synthesis techniques described were registered at room temperature with a Philips APT-15 diffractometer, using Cu K_α radiation in the $10 < 2\theta < 60$ range. The average crystallite size of the $LiVMoO_6$ phase was calculated from the broadening of the diffraction lines of (200) profile using Scherrer's equation. Infrared spectra of the products were registered in the range 1400–400 cm^{-1} using the KBr pellet technique on a Nicolet-320 FTIR spectrometer. The XPS measurements were carried out on an ESCALAB Mk II (VG Scientific) electron spectrometer with base vacuum in the analysis chamber of 10^{-8} Pa. The X-ray photoelectron spectra were recorded with Al K_α excitation source with photon energy of 1486.6 eV. The pass energy and slit widths of the electron analyzer were 20 eV and 6 mm, respectively, which gives a total instrumental resolution of 1.06 eV (as measured with the FWHM of $Ag3d_{5/2}$ photoelectron line). Energy calibration was performed, taking the C1s line at 285 eV as a reference phase. The experimental error of peak positions was in the range 0.1÷0.3 eV depending on the line intensity.

Results and discussion

Figure 2 present the X-ray diffraction patterns of a $LiVMoO_6$ phase obtained by different techniques (see Fig. 1). The diffraction patterns were indexed using "Index" software, assuming a C2/m symmetry that corresponds to the monoclinic citing of the brannerite structure [6]. The XRD data obtained were also compared with those existing in the literature [2, 5]. The diffraction patterns of the samples prepared by methods A, B contain mainly peaks characteristic for $LiVMoO_6$. There are also a few weak peaks that we could not index. According to the references [2, 5] the same peaks also appear in the diffraction patterns of the $LiVMoO_6$ phase. We suggest that the not indexed peaks probably belong to the unknown impurity phase. These results confirmed the optimal synthetic conditions for solid state and soft-combustion derived material. $LiVMoO_6$ as a main phase was also obtained employing melt quenching at different cooling rates (method C and D) (Fig. 2). The XRD patterns (curves A–D Fig. 2) show changes in intensity of diffraction line, which may be a result of a different preferential growth plane of the crystallites form by various synthesis ways. The calculated crystallite size of $LiVMoO_6$ ranges from 52 to 46 ± 2 nm depending on preparative manners.

In order to produce amorphous samples as precursors for preparation of $LiVMoO_6$ by crystallization of a glass (method E), we determined the glass formation region in the ternary Li_2O–V_2O_5–MoO_3 system. Two vitreous ranges were established in the system (Fig. 3): one of the compositions rich in MoO_3 (40–80 mol%) and the other of compositions with a high V_2O_5 content (50–100 mol%). Glasses containing Li_2O above 30 mol% were hygroscopic. The $LiVMoO_6$ was outside the glass formation regions obtained. A composition

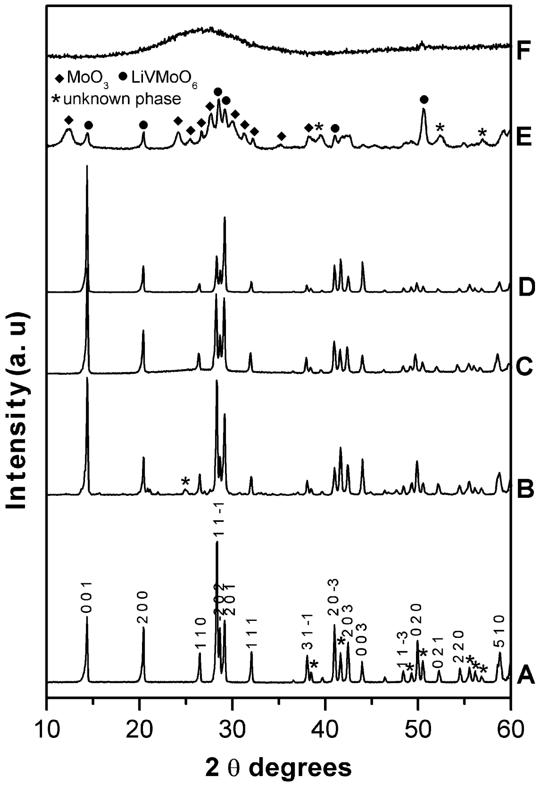

Fig. 2 X-ray diffraction patterns of $LiVMoO_6$ prepared by: **A**, solid state reaction; **B**, soft-combustion method; **C**, melt quenching (cooling rates–10^3 K/s); **D**, melt quenching (cooling rates 10^4–10^5 K/s); **E**, crystallization of a glass; **F**, glass sample with composition $20Li_2O \cdot 50V_2O_5 \cdot 30MoO_3$

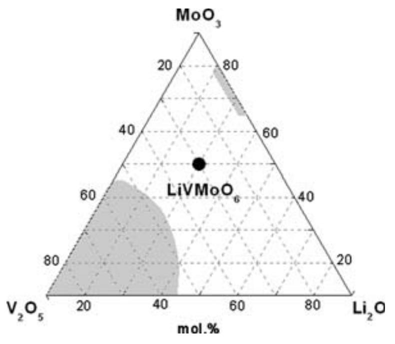

Fig. 3 Glass formation regions in the Li_2O–V_2O_5–MoO_3 system

inside the glass formation region (Fig. 3) subjected of heat treatment for 3 hours at 300°C is dominantly amorphous containing small amounts of crystalline $LiVMoO_6$ and MoO_3 (JSPDC-75-0912). The grain size of this sample is smallest-32 ± 2 nm as compared with calculated crystallites size of the phase obtained by other manners (see Fig. 1). This result shows that glass crystallization method is promising route for producing of polycrystalline and glass-crystalline materials with controlled particle size distribution. They will be subject of a special study in future.

Additional information on phase formation and structural features of $LiVMoO_6$ phase could be obtained by IR spectroscopy (Fig. 4). As one can see from the figure, the vibrational specta of samples prepared by methods A, B and C are very similar. They are in good agreement with the spectral data in the literature [2] and confirm the XRD result about formation of a crystalline $LiVMoO_6$. Amdouni et al. using factor group analysis [2] predicted (4Au + 9Bu) infrared active modes, in the spectrum of $LiVMoO_6$ but detailed interpretation of the bands situated between 900 cm^{-1} and 400 cm^{-1} was not made. We shall try to assign the observed bands having in mind the crystal structure of $LiVMoO_6$ and vibrational spectra of phases with similar building units [1, 7–9]. $LiVMoO_6$ crystallizes with ThTi2O6 brannerite-type structure composed of MeO_6 (Me = V, Mo) octahedra and isolated LiO_6 polyhedra (Fig. 5) [1, 6]. MeO_6 groups sharing both common edges form Me_2O_8 units and common corners rising Me–O–Me bridge. The bond distances ranging from 1.6839 to 2.1833 Å [1]. Taking into account the spectral data of Me_2O_8 units [7–9] the high intensity bands at 620 and 570 cm^{-1} in our spectra

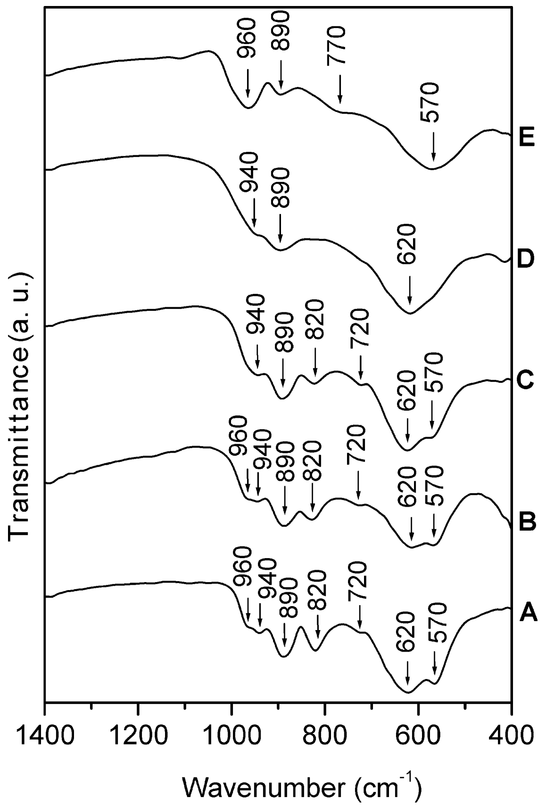

Fig. 4 IR spectra of $LiVMoO_6$ samples as a function of the synthesis methods

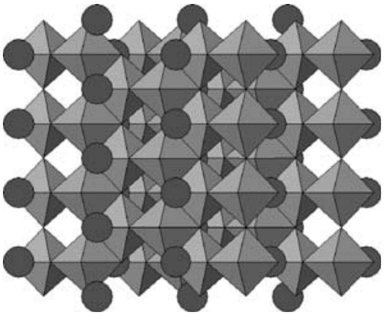

Fig. 5 Polyhedral view of the brannerite structure of $LiVMoO_6$ along the (101) plane

can be attributed to the asymmetric stretching mode of Me_2O_2 entity present in Me_2O_8 units. The shoulder at 720 cm^{-1} is due to symmetric vibration of the same entity [8]. The bands at 890 and 820 cm^{-1} are connected with vibrations of Me–O–Me bridges [8, 10–12]. High frequency bands at 960 and 940 cm^{-1} are associated to the terminal V = O and Mo = O bonds [2, 10–12]. There is some differences in the spectra of the samples prepared by melt quenching method at higher cooling rates (10^4–10^5 K/s) (curve D) as compared to $LiVMoO_6$ derived by other ways (Fig. 4). The absorption bands are broadened and low in intensity. These differences may be regarded as a result of change the size and/or morphology of crystallites, which was established by XRD analysis. Analogy discussion was made for influence of the heat treatment on IR spectra of MoO_3 [13]. More precise experiments are necessary to clarify this assumption.

Li1s, O1s, V2p and Mo3d spectra of all samples are presented in Fig. 6. Weak intensities of Li1s peak (curves A–D) at 56.0 ± 0.3 eV was observed due to the low photoionization cross section [14]. Its position is characteristic of the Li^+ oxidation state. [15, 16]. The $V2p_{3/2}$ photoelectron line of all products possesses a symmetric peak with a binding energy of 517.8 ± 0.1 eV typical of V^{5+} ions [15, 17]. The photoelectron Mo3d spectrum of all samples is characterized by a well-shaped narrow $Mo3d_{5/2}$ peak at 233.3 ± 0.1 eV which evidences presence of a molybdenum ions in a higher (Mo^{6+}) oxidation state only [18]. The O1s line of the $LiVMoO_6$ phase obtained by different methods exhibits a single highly symmetric peak positioned at 530.9 ± 0.1 eV which can be assigned to the V–O–V, V–O–Mo and Mo–O–Mo bonds present in its crystal structure [19].

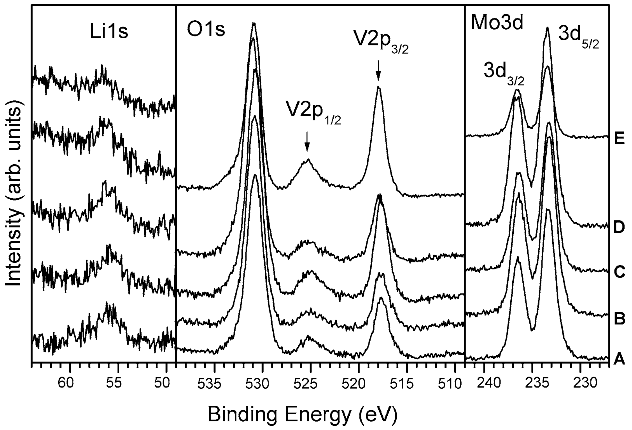

Fig. 6 Li1s, O1s, V2p and Mo3d photoelectron spectra of $LiVMoO_6$ samples as a function of the synthesis method

Conclusion

$LiVMoO_6$ phase was successfully synthesized applying two new methods: melt quenching and crystallization of a glass. They present some advantages compared to the known conventional solid-state reaction and soft-combustion synthesis as: the short preparation time and the smallest grain size (32 nm) of $LiVMoO_6$ powder. It is determined that glasses are stable up to 300 °C.

References

1. Liu R, Wang C, Jang L, Lee J (2002) Tamkang J Sci Eng 5:107
2. Amdouni N, Zarrouk H, Soulette F, Julien C (2003) J Mater Sci 13:2374
3. Liu RS, Wang CY, Drozd VA, Hu SF, Sheu HS (2005) Electrochem Solid State Lett 8(12):A650
4. Michael M, Fauzi A, Prabaharan S (2000) Int J Inorg Mater 2:261
5. Liang Y, Yang S, Yi Z, Sun J, Zhou Y (2005) J Mater Sci 40:5553
6. Run R, Wadsley A (1966) Acta Crust 21:974
7. Hanuza J, Labuda L (1981) J Raman Spectroscopy 11:231
8. Hanuza J, Macalik L (1987) Specrochem Acta 43A:361
9. Daturi M, Bursa G, Borel M, Leclaire A, Piagio P (1997) J Phys Chem B101:4358
10. Abello L, Husson E, Repelin Y, Lucazeau G (1983) Spectrochim Acta 39A:641
11. Barraclough C, Lewis J, Wyholm R (1959) J Chem Soc 3552
12. Seguin L, Figlarz M, Cavagnat R, Lassegues J (1995) Spectrochim Acta A51:1323
13. Eda K (1991) J Solid State Chem 95:64
14. Scofield JN (1976) J Electron Spectr Rel Phen 8:129
15. Bhuvaneswari M, Selvasekarapandian S, Fujihara S, Koji S (2006) Solid State Ionics 177:121
16. Atuchin VV, Kesler VG, Lisova IA, Pokrovsky LD, Pylneva NA, Yurkin AM (2003) Cryst Res Technol 38(10):896
17. Zimmermann R, Claessen R, Reinert F, Steiner P, Hüfner S (1998) J Phys: Condens Matter 10:5697
18. Van Oeffelen DAG, Van Hoof JHC, Schuit GCA (1985) J Catal 95:84
19. Barr T (1994) In: Modern ESCA, the principles and practice of X-ray photoelectron spectroscopy. CRS Press, Boca Raton, Fl